Journal of
Materials Chemistry C

RSC Publishing

PAPER

View Article Online
View Journal | View Issue

Published on 05 December 2012. Downloaded by Trinity College Dublin on 21/05/2013 08:32:47.

Computational testing of trivalent dopants in CeO_2 for improved high-κ dielectric behaviour

Cite this: *J. Mater. Chem. C*, 2013, **1**, 1093

Received 11th October 2012
Accepted 29th November 2012

DOI: 10.1039/c2tc00385f

www.rsc.org/MaterialsC

Patrick R. L. Keating,*[a] David O. Scanlon[b] and Graeme W. Watson[a]

Due to its high dielectric constant, large band gap, and very small lattice mismatch with Si, CeO_2 has been proposed as a promising candidate high-κ dielectric material. The performance of CeO_2 as a dielectric material, however, is severely limited due its propensity for facile reduction (oxygen vacancy formation), which causes a high interface state density, and subsequent decreased drain currents. In this article we use density functional theory (DFT) to screen for trivalent dopants which could decrease the concentration of defects in CeO_2 samples. We demonstrate that La and Y are the most soluble trivalent dopants in CeO_2, and can reduce the number of the electrons in the system both ionically (formation of [M_{Ce}–V_O–M_{Ce}] clusters) or to a lesser extent electronically (hole formation). La doping also increases the lattice constant of CeO_2, improving the lattice match with Si.

1 Introduction

Ceria (CeO_2) is a wide band gap insulator which has been widely utilized in catalysis where it can act as a catalyst itself,[1–4] or as a support material.[5–9] The properties that make CeO_2 attractive for catalytic processes are its high thermal stability and high oxygen storage capacity (OSC), which is ceria's ability to absorb oxygen in oxidizing environments and release oxygen under reducing conditions.[10–12] CeO_2 is also a promising candidate electrolyte in solid oxide fuel cells (SOFCs) operating in the intermediate temperature range ($\approx$600 to 1000 K).[13] It displays both ionic and electronic conductivity,[14] and it is known that both types of conductivity are influenced by the OSC since it governs the presence of intrinsic oxygen vacancies (V_O). Upon the formation of a V_O, two excess electrons will localize on two nearby cerium atoms, formally reducing them from Ce^{IV} to Ce^{III}.[15] The V_O will then act as a pathway for ionic diffusion[16] while the localized electrons are small polarons for electronic conductivity.[17] For SOFCs, it is important to have high ionic conductivity and a very low electronic conductivity, as electronic conductivity will short circuit the operation of the fuel cell. A common method for increasing the performance of CeO_2 electrolytes is the introduction of trivalent dopants, which introduce charge compensating vacancies (CCVs) without reducing the cerium ions.[18–27]

Recently, CeO_2 has been shown to be potentially useful in high-κ dielectric applications.[28–34] Currently HfO_2 is commonly used to replace SiO_2 in metal–oxide–semiconductor field-effect transistors (MOSFETs)[35–40] due to its moderate dielectric constant (14–18) and large band gap (5.8 eV).[38] However, there are some notable drawbacks to HfO_2 based MOSFETs. The main disadvantage is the large lattice mismatch between HfO_2 and the Si substrates, which can be as much as 6.39%.[41] Although stabilizing the cubic phase of HfO_2 by doping with yttrium can reduce this problem the lattice mismatch still remains high.[37,38] Furthermore, defects at the interface, such as Hf–Si bonds, can also degrade the operation of the MOSFET.[37] As a result of this, large leakage currents have been observed in HfO_2 MOSFETs.[37] In terms of a replacement for both SiO_2 and HfO_2, CeO_2 has been found to be a good candidate due to its high dielectric constant (23–52),[42–44] moderate band gap (2.76–3.60 eV),[45–47] small equivalent oxide thickness (EOT = 3.8 Å)[43] and low mismatch with the Si substrate ($\Delta d < 1\%$).[29]

To be effective for MOSFET applications, the interface state density (D_{it}) between CeO_2 and the Si substrate should be as low as possible as higher values of D_{it} are associated with decreased drain currents.[29] The formation energy of V_O in CeO_2 is quite low,[48] leading to the presence of Ce^{III} ions at the CeO_2–SiO_2 interface. The presence of such defects may cause higher values of D_{it}, and indeed it has been found that CeO_2 MOSFETs grown under oxygen-poor conditions have a greater leakage current than those grown under oxygen-rich conditions.[29] It is therefore clear that a mechanism for suppressing the interface state density in CeO_2 is necessary to maximize the potential of CeO_2 for high-κ dielectric applications.

In this article we employ the generalized gradient approximation with on-site Coulomb corrections (GGA + U) to investigate a series of intrinsic and extrinsic defects in CeO_2. We demonstrate: (i) the dominant intrinsic defect in CeO_2 is the V_O, which cannot be intrinsically compensated under Ce-rich/O-poor conditions, and can only be compensated at higher Fermi

[a] *School of Chemistry and CRANN, Trinity College Dublin, Dublin 2, Ireland. E-mail: keatinpr@tcd.ie*

[b] *University College London, Kathleen Lonsdale Materials Chemistry, Department of Chemistry, 20 Gordon Street, London WC1H 0AJ, UK*

Published on 05 December 2012. Downloaded by Trinity College Dublin on 21/05/2013 08:32:47.

energies (E_F) by cerium vacancies (V_{Ce}) under Ce-poor/O-rich conditions, (ii) La and Y doping can effectively compensate the electrons left behind upon V_O formation through the formation of [M_{Ce}–V_O–M_{Ce}] complexes, and (iii) the addition of La to CeO_2 increases the lattice constant, reducing the lattice mismatch with Si. We propose optimal growth conditions for La-doping to achieve maximally resistive CeO_2 with a low defect density.

2 Methods

All our DFT calculations were carried out using the VASP code,[49–51] utilizing GGA-PBE exchange–correlation functionals[52] with the projector augmented wave (PAW) method.[53] To describe the localized nature of both n-type and p-type defects in CeO_2, we apply $U = 5$ eV on the Ce_{4f},[54–57] and a $U = 5.5$ eV on the O_{2p}.[48] To avoid the problem of Paulay stress, the 12 atom unit cell of CeO_2 was optimized at a series of different volumes with a 500 eV plane wave cut-off and a 4 × 4 × 4 Monkhorst–Pack[58] k-point mesh. The resulting energy–volume data was fitted to the Murnaghan equation of state to give us the equilibrium lattice constant. Our approach yields a lattice constant of 5.477 Å which is within 1.2% of experiment, and a band gap of 2.51 eV,[48] which is underestimated compared to the experimental values as is common with GGA-DFT.[59] All the defects were modeled within a 2 × 2 × 2 (96 atom) expansion of the unit cell and a 2 × 2 × 2 Monkhorst–Pack k-point mesh. All calculations were spin polarized and deemed converged when the total force on each ion was less than 0.01 eV Å^{-1}.

The equilibrium concentration of a defect is determined by its formation energy. The formation energy of defect D with a charge state q is given by

$$\Delta H_f(D,q) = \left(E^{D,q} - E^{H}\right) + \sum_i n_i(E_i + \mu_i) + q(E_{Fermi} + \varepsilon^{H}_{VBM}) + E_{align}[q]. \quad (1)$$

E^H is the total energy of the stoichiometric host supercell and $E^{D,q}$ is the total energy of defective cell. The elemental reference energies are denoted by E_i. These are the energies of the constituent elements in their standard states, *i.e.*, $Ce_{(s)}$ and $O_{2(g)}$. n denotes the number of atoms that have been added to (positive value) or taken from (negative value) an external reservoir. E_f ranges from the valence band maximum (VBM) ($E_f = 0$ eV) to the calculated conduction band minimum (CBM) ($E_f = 2.51$ eV). ε^H_{VBM} is the VBM eigenvalue of the host bulk cell and $E_{align}[q]$ is a correction term which aligns the VBM of the bulk and defective cells and also corrects finite-size effects in calculations of charged defects. $E_{align}[q]$ is determined with the SXDEFECTALIGN code.[60] Tests comparing the correction scheme we have employed with similar correction schemes have demonstrated its excellent performance in the calculation of charged defects in finite-size supercells.[61] Furthermore, the SXDEFECT align code has been successfully applied to the description of charged defects in numerous systems.[62–66]

The chemical potentials, μ_i, represent specific equilibrium growth conditions, under the global constraint of the calculated enthalpy of formation of the host, *i.e.* CeO_2. Our calculated formation energy for ceria is $\Delta H_f(CeO_2) = \mu_{Ce} + 2\mu_O = -9.67$ eV. The upper limit for μ_O represents the Ce-poor/O-rich environment and is determined by the formation of gaseous oxygen: $\mu_{Ce} = -9.67$ eV, $\mu_O = 0$ eV. The lower limit of μ_O (Ce-rich/O-poor environment) is determined by the formation of Ce_2O_3: $\Delta H_f(Ce_2O_3) = -17.70$ eV, and hence we obtain $\mu_{Ce} = -6.39$ eV, $\mu_O = -1.64$ eV. For the calculation of doped CeO_2 we calculated the chemical potentials for the dopant cations using a method similar to the one described by Varley *et al.*,[67] where the boundary of the chemical potentials are set as the formation enthalpy of M_2O_3: $\Delta H_{M_2O_3} = 2\mu_M + 3\mu_O$ where M = Al, Ga, Sc, In, Tl, Y and La.

The thermodynamic transition/ionization levels of a defect, $\varepsilon_D(q/q')$, correspond to the Fermi-level energy at which the q and q' charge states of a defect are equal in energy:

$$\varepsilon_D(q/q') = \frac{\Delta H^f(D,q) - \Delta H^f(D,q')}{q' - q}. \quad (2)$$

3 Results and discussion

3.1 Intrinsic defects

The formation of point defects in a lattice can be compensated by ionic or electronic defects.[68] The intrinsic defects considered in this study include the positively charged V_O and Ce_i, which are electron compensated, as well as the negatively charged oxygen interstitial (O_i) and cerium vacancy (V_{Ce}) centres, which are hole compensated, as well as both Schottky and anion Frenkel defects. The energy of the excess electrons and holes are determined by the electron chemical potential (Fermi level).

Fig. 1 shows a plot of formation energy for all point defects under O-poor and O-rich conditions. Under O-poor growth conditions, it is clear that the dominant defect will be the V_O, which will not be compensated over the entire range of the band gap. V_O is a negative-U type defect, *i.e.* it exists only in the +2 and neutral charge states, consistent with the behaviour of V_O in a range of other wide band gap oxides.[69–75] The +2/0 ionization level is ~0.9 eV below the conduction band minimum, meaning that V_O is a *deep* donor, which is mediated by the localized Ce^{III} states present in the band gap.[54] Thus, under O-poor growth

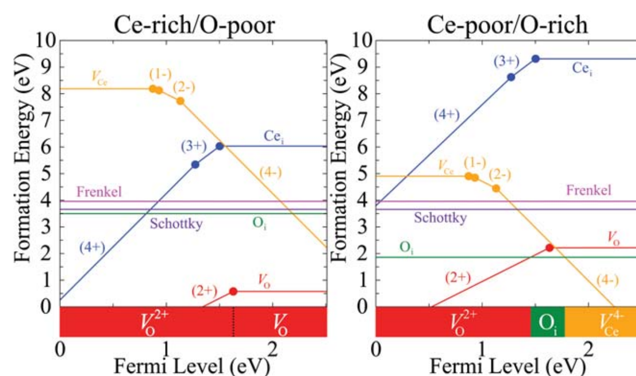

Fig. 1 Formation energies for intrinsic defects under O-poor conditions (left panel) and O-rich (right panel) conditions. 'The coloured regions at the bottom indicate which defect is energetically preferred.

This journal is © The Royal Society of Chemistry 2013

Published on 05 December 2012. Downloaded by Trinity College Dublin on 21/05/2013 08:32:47.

conditions, the number of V_O present will most likely produce large D_{it}, which will be detrimental to high-κ applications.

In an O-rich growth environment, V_O is the most stable defect up to 1.03 eV below the CBM, whereafter the interstitial peroxide (dumbell O_i, similar to that formed in many wide band gap oxides[48,66,76–82]), followed by the V_{Ce} in the −4 charge state, start to dominate. Although at higher E_F the electrons formed upon V_O formation would be compensated, it is highly unlikely that the E_F could ever be raised high enough, due to the polaronic nature of reduced Ce,[54] which means that the Fermi level will be trapped near the Ce^{III} states in the band gap. Therefore, the much higher formation energy of V_O in this growth regime is the explanation for the lower D_{it} from samples grown in an O-rich growth environment.[29] There will be, however, a considerable amount of V_O present in the system under O-rich conditions,[48] which needs to be significantly reduced for optimum performance.

3.2 Trivalent dopants

At this juncture, it is instructive to rationalize what research in the field of catalysis has learned about the behaviour of dopants in CeO_2. For instance, both divalent and trivalent dopants will form charge compensating vacancy (CCV) to counteract the charge imbalance, and will also experience lattice relaxations which forms weakly bound or undercoordinated lattice oxygen, lowering the V_O formation energy,[83–86] while pentavalent dopants donate one electron to the Ce lattice, creating new electronic states.[87] Trivalent dopants are regularly used to create oxygen vacancies in CeO_2 for SOFC applications, where the V_O act as diffusion pathways, but they are not noted for increasing the reducibility of CeO_2 and may even reduce it.[88,89]

A trivalent dopant can enter the CeO_2 lattice as either a substitutional defect (M_{Ce}) or as an interstitial, M_i. Previous theoretical studies[48,90] and many years of experimental characterization of trivalently doped CeO_2 for SOFC applications have demonstrated that cations interstitials are highly unlikely to be present in CeO_2, and so we have considered only substitutional defects in our calculations. We calculated a range of 3+ dopants (Sc, Y, La, Al, Ga, In, Tl), testing both ionic compensation ([M_{Ce}–V_O–M_{Ce}] formation) and electronic compensation by hole formation ([M_{Ce}– $O_O^{\bullet}$]).

From an extensive search of configurations of the [M_{Ce}–V_O–M_{Ce}] complexes, we found that the lowest energy structure depends on the ionic radius of the dopant ions. The ionic radii of Al^{III} and Ga^{III} are much smaller than that of Ce^{IV}, 1.11 Å, resulting in the configuration seen in Fig. 2(a), with the CCV nearest-neighbour to one of the dopants. As the ionic radius of the dopant increases, but remains smaller than Ce^{IV}, the most stable configuration has a CCV nearest neighbour to both the dopant ions, as seen in Fig. 2(b). Finally for La^{III}, which has a larger ionic radius than Ce^{IV}, the CCV is now next-nearest neighbour to the two dopants (Fig. 2(c)). From the range of dopants considered, La was found to be the most soluble acceptor defect, with Y the next most soluble with the energies for the complex shown in Fig. 3 (dashed lines).

The formation energies for [M_{Ce}– $O_O^{\bullet}$] defects are also shown in Fig. 3 (solid lines). Once again, La and Y are the most soluble dopants. All M_{Ce} dopants formed localized oxygen holes (polarons) neighbouring the dopant, and thus the corresponding 0/−1 transition levels are deep in the band gap. The correct modeling of this requires the DFT self-interaction error be canceled and hence this is why we apply $+U = 5.5$ eV to the O 2p states. This behaviour is to be expected for a material with an O

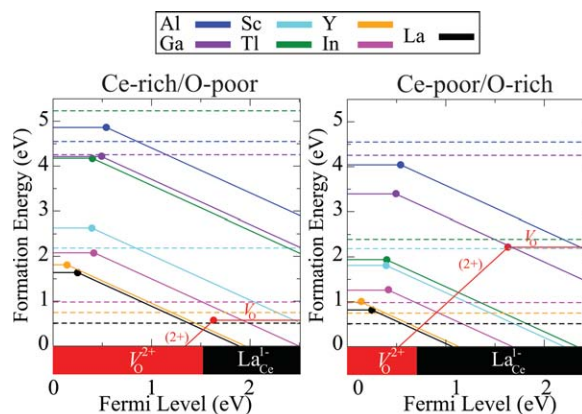

Fig. 3 Formation energies for trivalent dopants in CeO_2 under O-poor conditions (left panel) and O-rich (right panel) conditions. The full lines indicate the M_{Ce} defects, with the dashed lines indicating the [M_{Ce}–V_O–M_{Ce}] formation energies. 'The coloured regions at the bottom indicate which defect is energetically preferred.

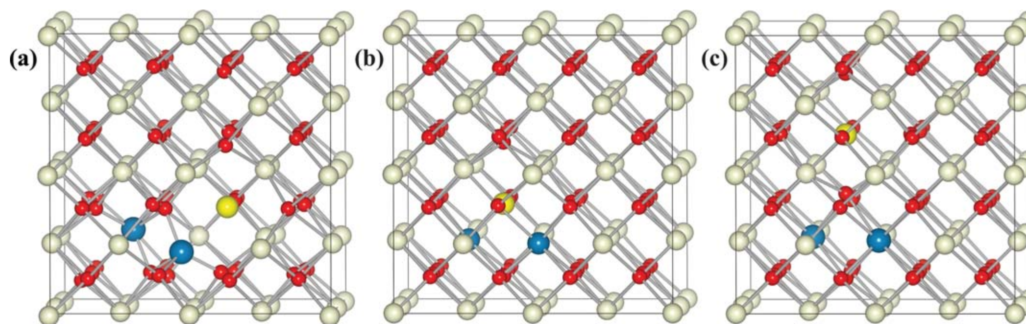

Fig. 2 The converged structures [M_{Ce}–V_O–M_{Ce}] defect clusters in CeO_2 with the charge compensating vacancy (a) nearest neighbor to one dopant (Al, Ga), (b) nearest neighbor to both dopants (Sc, Tl, Y, In) and (c) next nearest neighbor to both dopants (La). Ce ions are represented by the white spheres, O ions by the red spheres and the dopant ions by the blue spheres. The position of the charge compensating vacancy (CCV) is represented by the yellow sphere.

Published on 05 December 2012. Downloaded by Trinity College Dublin on 21/05/2013 08:32:47.

2p dominated VB[91,92] and has been observed in other oxide materials.[93,94] The La_{Ce}^{1-} and Y_{Ce}^{1-} charge states cross the V_O^{2+} charge state near the middle of the band gap, indicating that La and Y doping can compensate the electrons from V_O formation, pinning E_F in the band gap.

Although in all cases the formation energy of M_{Ce} was lower than the formation energy of the $[M_{Ce}–V_O–M_{Ce}]$, this comparison is slightly misleading, as there are different numbers of M in each defect. To determine whether ionic (CCV) or electronic (oxygen hole) compensation of the dopants is preferable, we have calculated the relative stability of $[M_{Ce}–V_O–M_{Ce}]$ and $[M_{Ce}–O_O^{\bullet}]$ from the equation: $2\Delta H_f[M_{Ce}–O_O^{\bullet}] \xrightarrow{\Delta E} \Delta H_f[M_{Ce}–V_O–M_{Ce}] + \frac{1}{2}E(O_2)$. The results of these calculations, shown in Table 1, are all negative which indicates that upon the introduction of trivalent dopants in CeO_2, the formation of the CCV is spontaneous and hence ionic compensation is preferable to electronic compensation.

To determine how strongly bound the dopant cations and CCV are, we have calculated the binding energy of these complexes, using: $E_b = \Delta H_f(V_O^{2+}) + 2\Delta H_f(M_{Ce}^{1-}) - \Delta H_f[M_{Ce}–V_O–M_{Ce}]$. If the value of E_b is positive, then the dopant will preferentially form the $[M_{Ce}–V_O–M_{Ce}]$ clusters instead of isolated V_O and M_{Ce} defects, with the results of this analysis shown in Table 2. The binding energy is positive in all cases, hence the thermodynamic driving force is for $[M_{Ce}–V_O–M_{Ce}]$ formation.

Under O-rich growth conditions, the energy to dope CeO_2 with La or Y is lower than the formation energy of the V_O, indicating that both dopants will act as an effective electron *killer*, therefore reducing the D_{it} which will be very beneficial for high-κ dielectric applications. Interestingly, as the ionic radii of La^{III} (1.16 Å) and Y^{III} (1.02 Å) are larger than that of Ce^{IV} (0.97 Å), the incorporation of La and Y could increase the lattice constant of CeO_2. To check this effect, we have carried out a series of constant volume optimizations of a 2 × 2 × 2 supercell, containing a $[M_{Ce}–V_O–M_{Ce}]$ cluster ($Ce_{30}M_2O_{63}$). The resulting energy–volume data was fitted to the Murnaghan equation of state to obtain the new equilibrium lattice volume for the doped supercells. It was found that the lattice constant for La doped CeO_2 is increased by 0.285%, whereas in Y doped CeO_2 the lattice constant actually decreased by 0.08%. This is because the expansion associated with the dopant cations is counteracted by a contraction due to the CCV. Marrocchelli *et al.* determined that a trivalent dopant must have an ionic radius greater than 1.03 Å to cause overall expansion of the CeO_2 lattice.[95] Therefore La doping will decrease the lattice mismatch between CeO_2 (5.41 Å)[96] and Si (5.43 Å)[97] even further while Y doping would increase it making La the most effective dopant for MOSFET applications out of those studied in this report.

Table 1 The stability of $[M_{Ce}–V_O–M_{Ce}]$ defect clusters compared to $[M_{Ce}–O_O^{\bullet}]$. All values are given in eV

Dopant	Al	Ga	In	Tl	Sc	Y	La
ΔE (O-poor)	−4.86	−3.87	−2.87	−2.81	−2.77	−2.57	−2.46
ΔE (O-rich)	−6.51	−5.51	−4.51	−4.46	−4.41	−4.21	−4.10

Table 2 The binding energies for $[M_{Ce}–V_O–M_{Ce}]$ defect clusters. All values are given in eV

Dopant	Al	Ga	In	Tl	Sc	Y	La
E_b	3.58	2.29	1.33	1.23	1.00	0.48	0.59

4 Conclusions

In summary, we have studied a range of trivalent dopants in CeO_2 as a means to lower the inherent density of electrons in the system, caused by V_O formation. Our calculations predict that La and Y are the best *electron killer* defects, being the most soluble trivalent dopants in CeO_2, compensating electrons ionically through $[M_{Ce}–V_O–M_{Ce}]$ formation. The incorporation of La increases the lattice constant of CeO_2, lowering the already small lattice mismatch between CeO_2 and Si. Growth of La-doped CeO_2 under Ce-poor/O-rich conditions is expected to be optimal for production of highly resistive CeO_2. These results open up the possibility of La-doped CeO_2 as a replacement for SiO_2 in high-κ dielectric applications.

Acknowledgements

This work was supported by Science Foundation Ireland through the Research Frontiers Programme (grant numbers 08/RFP/MTR1044 and 09/RFP/MTR2274). Calculations were performed on the Lonsdale and Kelvin supercomputers as maintained by TCHPC, and the Stokes supercomputer as maintained by ICHEC. D. O. S. is grateful to the Ramsay Memorial Trust and University College London for the provision of a Ramsay Fellowship, acknowledges the use of the UCL Legion High Performance Computing Facility, and associated support services, in the completion of this work. The authors also acknowledge membership of the UK's HPC Materials Chemistry Consortium, which is funded by EPSRC grant EP/F067496.

References

1 J. X. Guo, S. H. Yuan, M. C. Gong, L. Zhang, J. Zhang, L. M. Zhao and Y. Q. Chen, *Acta Chimica Sinica*, 2007, **10**, 937–942.
2 K. Krishna, A. Bueno-Lopez, M. Makkee and J. A. Moulijn, *Top. Catal.*, 2007, **42–43**, 221–228.
3 J. G. Nunan, M. J. Cohn and J. T. Dormer, *Catal. Today*, 1992, **14**, 277–291.
4 K. Zhou, X. Wang, X. Sun, Q. Peng and Y. Li, *J. Catal.*, 2005, **229**, 206–212.
5 W. L. Deng, C. Carpenter, N. Yi and M. Flytzani-Stephanopoulos, *Top. Catal.*, 2007, **44**, 199–208.
6 R. Si and M. Flytsani-Stephanopoulos, *Angew. Chem., Int. Ed.*, 2008, **47**, 2884–2887.
7 P. Panagiotopoulou, J. Papavasiliou, G. Avgouropoulos and T. Ioannides, *Chem. Eng. J.*, 2007, **134**, 16–22.
8 M. F. Camellone and S. Fabris, *J. Am. Chem. Soc.*, 2009, **131**, 10473–10483.

This journal is © The Royal Society of Chemistry 2013

Published on 05 December 2012. Downloaded by Trinity College Dublin on 21/05/2013 08:32:47.

9 M. V. Ganduglia-Pirovano, C. Popa, J. Sauer, H. Abbott, A. Uhl, M. Baron, D. Stacchiola, O. Bondarchuk, S. Shaikhutdinov and H.-J. Freund, *J. Am. Chem. Soc.*, 2010, **132**, 2345–2349.
10 M. A. Henderson, C. L. Perkins, M. H. Engelhard, S. Thevuthasan and C. H. F. Peden, *Surf. Sci.*, 2003, **526**, 1–18.
11 Z. X. Yang, T. K. Woo, M. Baudin and K. Hermansson, *J. Chem. Phys.*, 2004, **120**, 7741–7749.
12 D. A. Andersson, S. I. Simak, N. V. Skorodumova, I. A. Abrikosov and B. A. Johansson, *Appl. Phys. Lett.*, 2007, **90**, 031909.
13 D. J. L. Brett, A. Atkinson, N. P. Brandon and S. J. Skinner, *Chem. Soc. Rev.*, 2008, **37**, 1568–1578.
14 H. F. Wang, X. Q. Gong, Y. L. Guo, Y. Guo, G. Z. Lu and P. Hu, *J. Phys. Chem. C*, 2009, **113**, 10229–10232.
15 M. Nolan, S. Grigoleit, D. C. Sayle, S. C. Parker and G. W. Watson, *Surf. Sci.*, 2005, **576**, 217–229.
16 H. Hayashi, R. Sagawa, R. Inaba and K. Kawamura, *Solid State Ionics*, 2000, **131**, 281–290.
17 T. Kudo and H. Obayashi, *J. Electrochem. Soc.*, 1976, **123**, 415.
18 Y. P. Fu, C. W. Tseng and P. C. Peng, *J. Eur. Ceram. Soc.*, 2008, **28**, 85–90.
19 V. Esposito, M. Zunic and E. Traversa, *Solid State Ionics*, 2009, **180**, 1069–1075.
20 S. Kuharuangrong, *J. Power Sources*, 2007, **171**, 506–510.
21 B. Rambabu, S. Ghosh and J. Hrudananda, *J. Mater. Sci.*, 2006, **41**, 7530–7536.
22 S. Sen, H. J. Avila-Paredes and S. Kim, *J. Mater. Chem.*, 2008, **18**, 3915–3917.
23 B. Zhu, X. Liu, Z. Zhu and R. Ljungberg, *Int. J. Hydrogen Energy*, 2008, **33**, 3385–3392.
24 S. Zha, C. Xia and G. Meng, *J. Power Sources*, 2002, **115**, 44–48.
25 X. Sha, Z. Lu, X. Huang, J. Miao, Z. Ding, X. Xin and W. Su, *J. Alloys Compd.*, 2007, **428**, 59–64.
26 X. Guan, H. Zhou, Z. Liu, Y. Wang and J. Zhang, *Mater. Res. Bull.*, 2008, **43**, 1046–1054.
27 M. Burbano, D. Marrocchelli, B. Yildiz, H. L. Tuller, S. T. Norberg, S. Hull, P. A. Madden and G. W. Watson, *J. Phys.: Condens. Matter*, 2011, **23**, 255402.
28 F.-C. Chiu, S.-Y. Chen, C.-H. Chen, F.-W. Chen, H.-S. Huang and H.-L. Hwang, *Jpn. J. Appl. Phys.*, 2009, **48**, 04C014.
29 Y. Nishikawa, T. Yamaguchi, M. Yoshiki, H. Satake and N. Fukushima, *Appl. Phys. Lett.*, 2002, **81**, 4386.
30 C.-H. Chen, I. Y.-K. Chang, J. Y.-M. Lee and F.-C. Chiu, *Appl. Phys. Lett.*, 2008, **92**, 043507.
31 W.-H. Kim, M.-K. Kim, W. J. Maeng, J. Gaineau, V. Pallem, C. Dussarrat, A. Noori, D. Thompson, S. Chu and H. Kim, *J. Electrochem. Soc.*, 2011, **158**, G169–G172.
32 M.-H. Tang, Y.-C. Zhou, X.-J. Zheng, Q.-P. Wei, C.-P. Cheng, Z. Ye and Z.-S. Hu, *Trans. Nonferrous Met. Soc. China*, 2007, **17**, s741–s746.
33 F.-C. Chiu and C.-M. Lai, *J. Phys. D: Appl. Phys.*, 2010, **43**, 075104.
34 F.-C. Chiu, *Electrochem. Solid-State Lett.*, 2008, **11**, H135–H137.
35 Y. Zhao, *Materials*, 2012, **5**, 1413–1438.
36 E. J. Kim, M. Shandalov, K. C. Saraswat and P. C. McIntyre, *Appl. Phys. Lett.*, 2011, **98**, 032108.
37 J. Y. Dai, P. F. Lee, K. H. Wong, H. L. W. Chan and C. L. Choy, *J. Appl. Phys.*, 2003, **94**, 912.
38 D. W. McNeill, S. Bhattacharya, H. Wadsworth, F. H. Ruddel, S. J. Mitchell, B. M. Armstrong and H. S. Gamble, *J. Mater. Sci.: Mater. Electron.*, 2008, **19**, 119–123.
39 Y. Aoki, T. Kunitake and A. Nakao, *Chem. Mater.*, 2005, **17**, 450–458.
40 G. D. Wilk, R. M. Wallace and J. M. Anthony, *J. Appl. Phys.*, 2001, **89**, 5243.
41 J. Wang, H. P. Li and R. Stevens, *J. Mater. Sci.*, 1992, **27**, 5397–5430.
42 N. V. Skorodumova, R. Ahuja, S. I. Simak, I. A. Abrikosov, B. Johansson and B. I. Lundqvist, *Phys. Rev. B: Condens. Matter*, 2001, **64**, 115108.
43 Y. Nishikawa, N. Fukushima, N. Yasuda, K. Nakayama and S. Ikegawa, *Jpn. J. Appl. Phys.*, 2002, **41**, 2480–2483.
44 T. Yamamoto, H. Momida, T. Hamada, T. Uda and T. Ohno, *Thin Solid Films*, 2005, **486**, 136–140.
45 G. Magesh, B. Viswanathan, R. P. Viswanath and T. K. V. Varadarajan, *Indian J. Chem., Sect. A: Inorg., Bio-inorg., Phys., Theor. Anal. Chem.*, 2009, **46**, 480–488.
46 S. Sathyamurthy, K. J. Leonard, R. Davestani and M. P. Paranthaman, *Nanotechnology*, 2005, **16**, 1960–1964.
47 S. Debnath, M. R. Islam and M. S. R. Khan, *Bull. Mater. Sci.*, 2007, **30**, 315–319.
48 P. R. L. Keating, D. O. Scanlon, B. J. Morgan, N. M. Galea and G. W. Watson, *J. Phys. Chem. C*, 2012, **116**, 2443–2452.
49 G. Kresse and J. Hafner, *Phys. Rev. B: Condens. Matter*, 1994, **49**, 14251–14269.
50 G. Kresse and J. Furthmuller, *Phys. Rev. B: Condens. Matter*, 1996, **54**, 11169–11186.
51 G. Kresse and J. Furthmuller, *Comput. Mater. Sci.*, 1996, **6**, 12–50.
52 K. E. M. Perdew and J. P. Burke, *Phys. Rev. Lett.*, 1996, **77**, 3865–3868.
53 P. E. Blochl, *Phys. Rev. B: Condens. Matter*, 1994, **50**, 17953–17979.
54 P. R. L. Keating, D. O. Scanlon and G. W. Watson, *J. Phys.: Condens. Matter*, 2009, **21**, 405502.
55 N. M. Galea, D. O. Scanlon, B. J. Morgan and G. W. Watson, *Mol. Simul.*, 2009, **35**, 577–583.
56 M. Nolan, S. C. Parker and G. W. Watson, *Surf. Sci.*, 2005, **595**, 223–232.
57 M. Nolan, S. C. Parker and G. W. Watson, *Surf. Sci.*, 2006, **600**, L175–L178.
58 H. J. Monkhorst and J. D. Pack, *Phys. Rev. B: Solid State*, 1976, **13**, 5188–5192.
59 K. G. Godinho, G. W. Watson, A. Walsh, A. J. H. Green, D. J. Payne, J. Harmer and R. G. Egdell, *J. Mater. Chem.*, 2008, **18**, 2798–2806.
60 C. Freysoldt, J. Neugebauer and C. G. Van de Walle, *Phys. Rev. Lett.*, 2009, **102**, 016402.
61 H.-P. Komsa, T. Rantala and A. Pasquarello, *Phys. B*, 2012, **407**, 3063–3067.

This journal is © The Royal Society of Chemistry 2013

Published on 05 December 2012. Downloaded by Trinity College Dublin on 21/05/2013 08:32:47.

62 D. O. Scanlon and G. W. Watson, *J. Mater. Chem.*, 2011, **21**, 3655–3663.
63 D. O. Scanlon and G. W. Watson, *J. Phys. Chem. Lett.*, 2010, **1**, 3195–3199.
64 Q. Yan, A. Janotti, S. Matthias and C. G. Van de Walle, *Appl. Phys. Lett.*, 2012, **100**, 142110.
65 M. Burbano, D. O. Scanlon and G. W. Watson, *J. Am. Chem. Soc.*, 2011, **133**, 15065–15072.
66 D. O. Scanlon, A. B. Kehoe, G. W. Watson, M. O. Jones, W. I. F. David, D. J. Payne, R. J. Egdell, P. P. Edwards and A. Walsh, *Phys. Rev. Lett.*, 2011, **107**, 246402.
67 J. B. Varley, A. Janotti and C. G. Van de Walle, *Phys. Rev. B: Condens. Matter Mater. Phys.*, 2010, **81**, 245216.
68 C. R. A. Catlow, A. A. Sokol and A. Walsh, *Chem. Commun.*, 2011, **47**, 3386–3388.
69 S. Lany and A. Zunger, *Phys. Rev. B: Condens. Matter Mater. Phys.*, 2008, **78**, 235104.
70 F. Oba, A. Togo, I. Tanaka, J. Paier and G. Kresse, *Phys. Rev.B: Condens. Matter Mater. Phys.*, 2008, **77**, 245202.
71 S. Lany and A. Zunger, *Phys. Rev. B: Condens. Matter Mater. Phys.*, 2010, **81**, 205209.
72 A. K. Singh, A. Janotti, M. Scheffler and C. G. Van de Walle, *Phys. Rev. Lett.*, 2008, **101**, 055502–055504.
73 J. B. Varley, J. R. Weber, A. Janotti and C. G. V. de Walle, *Appl. Phys. Lett.*, 2010, **97**, 142106.
74 P. Agoston, K. Albe, R. M. Nieminen and M. J. Piska, *Phys. Rev. Lett.*, 2009, **103**, 245501.
75 S. Limpijumnong, P. Reunchan, A. Janotti and C. G. Van de Walle, *Phys. Rev. B: Condens. Matter Mater. Phys.*, 2009, **80**, 193202.
76 A. Janotti and C. G. Van de Walle, *Phys. Rev. B: Condens. Matter Mater. Phys.*, 2007, **76**, 165202.
77 A. A. Sokol, S. A. French, S. T. Bromley, C. R. A. Catlow, H. J. J. van Dam and P. Sherwood, *Faraday Discuss.*, 2007, **134**, 267–282.
78 A. A. Sokol, A. Walsh and C. R. A. Catlow, *Chem. Phys. Lett.*, 2010, **492**, 44–48.
79 B. J. Morgan and G. W. Watson, *Phys. Rev. B: Condens. Matter Mater. Phys.*, 2009, **80**, 233102.
80 S. Na-Phattalung, M. F. Smith, K. Kim, M.-H. Du, S.-H. Wei, S. B. Zhang and S. Limpijumnong, *Phys. Rev. B: Condens. Matter Mater. Phys.*, 2006, **73**, 125205.
81 K. G. Godinho, A. Walsh and G. W. Watson, *J. Phys. Chem. C*, 2008, **113**, 439–448.
82 P. Agoston, C. Korber, A. Klein, M. J. Puska, R. M. Nieminen and K. Albe, *J. Appl. Phys.*, 2010, **108**, 053511.
83 D. O. Scanlon, B. J. Morgan and G. W. Watson, *Phys. Chem. Chem. Phys.*, 2011, **13**, 4279–4284.
84 A. B. Kehoe, D. O. Scanlon and G. W. Watson, *Chem. Mater.*, 2011, **23**, 4464–4468.
85 G. Dutta, U. V. Waghmare, T. Baidya, M. S. Hegde, K. R. Priolkar and P. R. Sarode, *Chem. Mater.*, 2006, **18**, 3249.
86 G. Dutta, U. V. Waghmare, T. Baidya, M. S. Hegde, K. R. Priolkar and P. R. Sarode, *Catal. Lett.*, 2006, **108**, 165–172.
87 M. Nolan, *Chem. Phys. Lett.*, 2010, **492**, 115–118.
88 W. Zając and J. Molenda, *Solid State Ionics*, 2011, **192**, 163–167.
89 H. Yahiro, K. Eguchi and H. Arai, *Solid State Ionics*, 1989, **36**, 71–75.
90 X. Wang, M. Shen, J. Wang and S. Fabris, *J. Phys. Chem. C*, 2010, **114**, 10221–10228.
91 D. O. Scanlon, A. Walsh, B. J. Morgan, M. Nolan, J. Fearon and G. W. Watson, *J. Phys. Chem. C*, 2007, **111**, 7971–7979.
92 O. F. Schirmer, *J. Phys.: Condens. Matter*, 2006, **18**, R667–R704.
93 D. O. Scanlon, A. Walsh, B. J. Morgan and G. W. Watson, *e-J. Surf. Sci. Nanotechnol.*, 2009, **7**, 395–404.
94 M. Nolan and G. W. Watson, *J. Chem. Phys.*, 2006, **125**, 144701.
95 D. Marrocchelli, S. R. Bishop, H. L. Tuller and B. Yildiz, *Adv. Funct. Mater.*, 2012, **22**, 1958–1965.
96 M. Yashima, S. Kobayashi and T. Yasui, *Solid State Ionics*, 2006, **177**, 211–215.
97 A. Kohno, N. Aomine, Y. Soejima and A. Okazaki, *Jpn. J. Appl. Phys.*, 1994, **33**, 5073.

This journal is © The Royal Society of Chemistry 2013